Effect of Coldrolling and Cryorolling on Microstructure and Properties of UFG IF Steel Processed by ECAP

6.1 Microstructure

As-received IF steel (Figure 3.1a) shows equiaxed ferrite grains of average grain size 57.6±21 µm, domain size of 164 nm and low amount of elastic stored energy of 26.9 Joule/mole (Table 6.1). When the material is ECAPed, the elongated subgrain structures with scattered dislocations are formed (Figures 6.1(a),6.2(a)) but interior of a few subgrains are dislocation free. Severe plastic deformation by ECAP process refines the grain to average size of 196 nm. Domain size decreases to ~41 nm and lattice strain increases to 0.21% (Table 6.1). On further deformation of the ECAPed sample by cold rolling to 90% (ECAP-12-CR-90) reduction in area, the material is dynamically recovered with dislocations arranging in the form of cells (shown by arrow in Figure 6.2(b)) and dislocation tangles (indicated by A). The cell walls of thick dislocation boundaries of size 204 nm are also observed at some places. Most of the cell interiors are dislocation free (Figure 6. 3(b)).
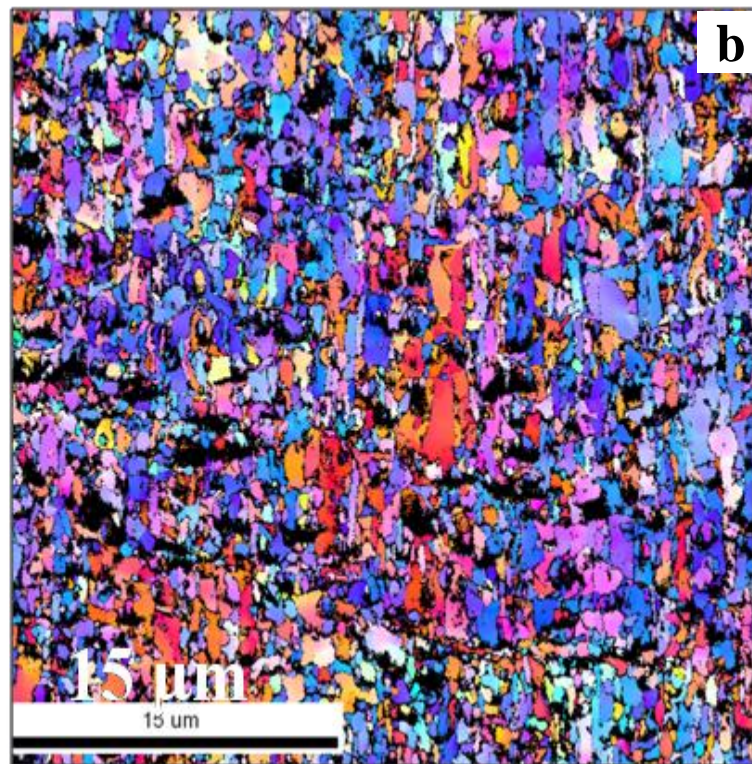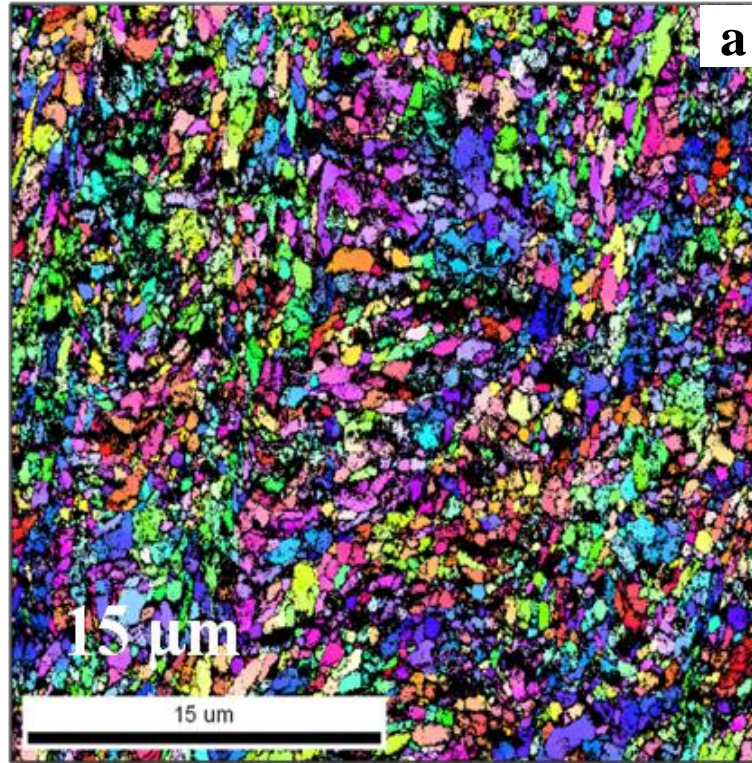
Figure 6.1: [001] Inverse pole figure (IPF) maps for (a) ECAP-12 and (b) ECAP-12-CR-90 for normal direction.
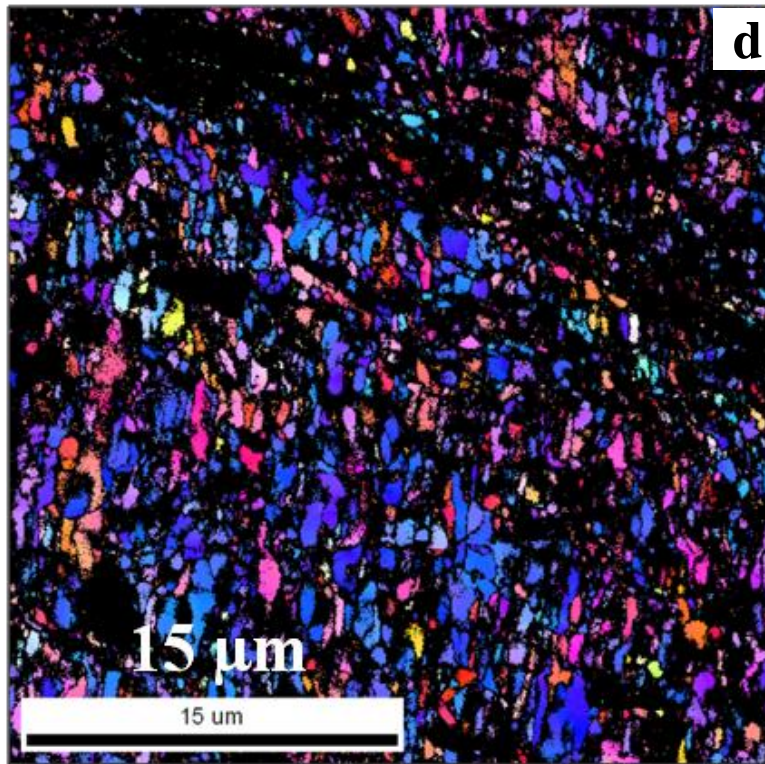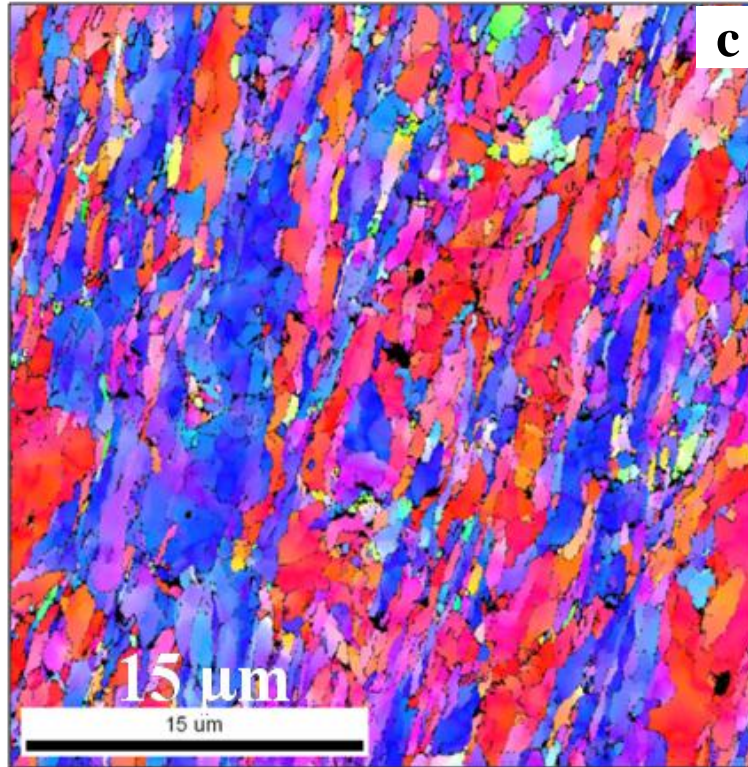
Figure 6.1: [001] IPF maps for (c) ECAP-12-CRR-70, (d) ECAP-12-CRR-96,

The domain size reduces further to ~34 nm and lattice strain increases to 0.23%. When the ECAPed billet is cryorolled to 70% reduction in area i.e. in case of ECAP-12-CRR-70 sample, the domain size becomes 42.7 nm and the lattice strain decreases marginally to 0.19%. The elongated grains are parallel mainly to [111] and [001] orientations (Figure 6.2(c)) of normal direction. The bright field image of this material shows that a large number of dislocations are accumulated at the grain boundaries of 138 nm (Figure 6.3(c)). The band extinction contours also exist at and near the grain boundary region. The grain size and the elastic stored energy are lower than that of ECAP-12-CR-90. When ECAPed samples are further cryorolled to 96% reduction in area, a mixture of equiaxed and elongated grain structures of 127 nm are formed (Figure 6.2(d)). However at high magnification TEM image shows that the diffuse cell boundaries have formed with a large scattered dislocation network in the interior of grains (Figure 6.3(d)). The domain size decreases from 41 nm to 36 nm. The elastic stored energy increases and it is higher than that of ECAP-12CR-90 and ECAP-12-CRR-70.

Table 6.1: Microstructural parameters of post ECAPed deformed IF steel samples.

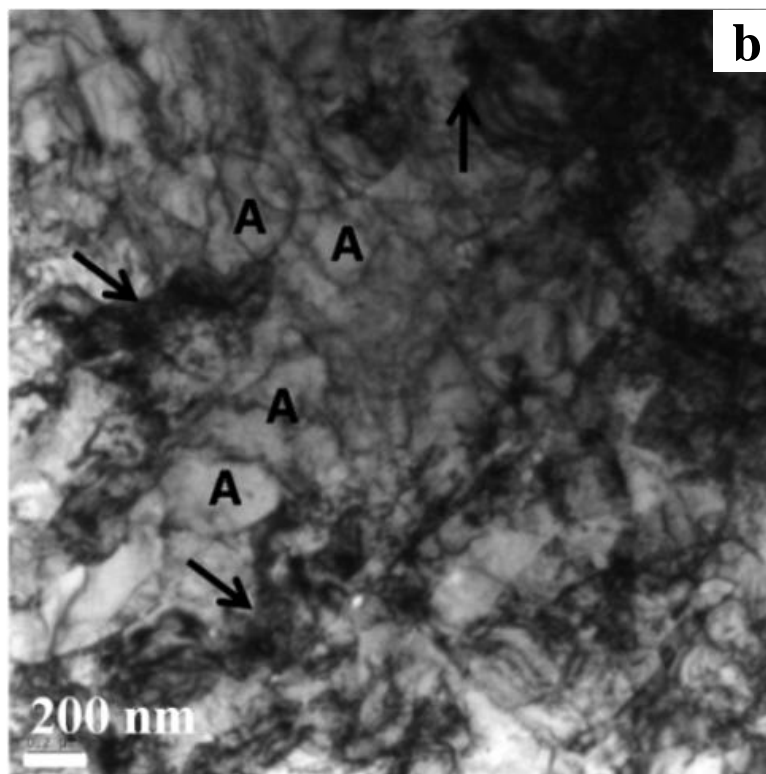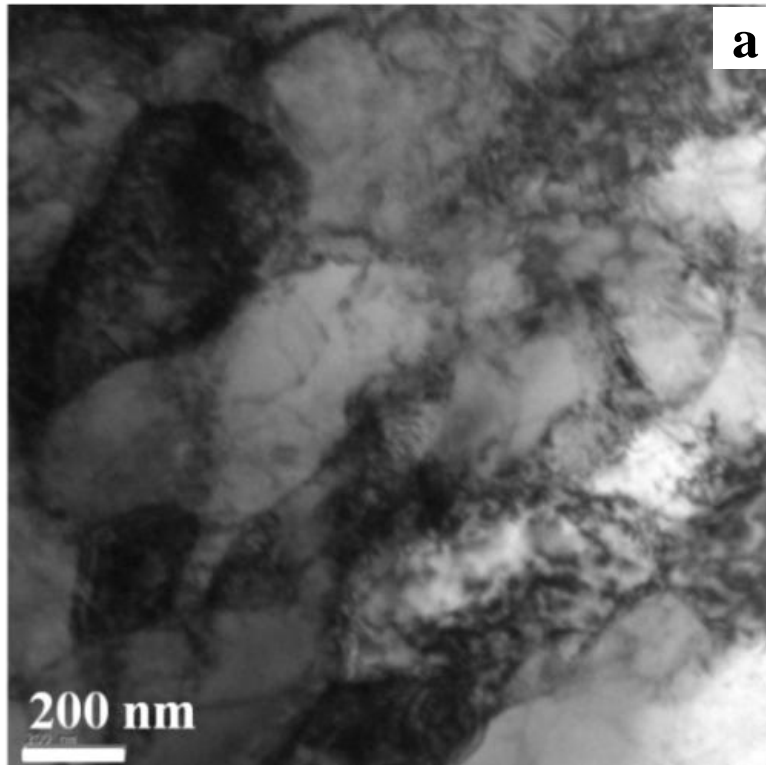| Sample	Domain size (nm)	Grain size (nm)	Strain (%)	Elastic stored energy (Joule/mole)	HAGB (%)	LAGB (%)	Misorientation angle (º)	Hardness (VHN)
As-received	164	57.6 μm	0.12	26.9	88.4	11.6	37	174±7.5
ECAP-12	41	196	0.21	50.9	34.5	65.5	15.8	300±3
ECAP-12-CR-90	34	204	0.23	57	58.3	41.7	25.9	524±25
ECAP-12-CRR-70	42.7	138	0.19	51.4	49.2	50.8	22.3	390.7±4.3
ECAP-12-CRR-96	36	127	0.23	60	60.8	39.2	25.7	530.3±0.5

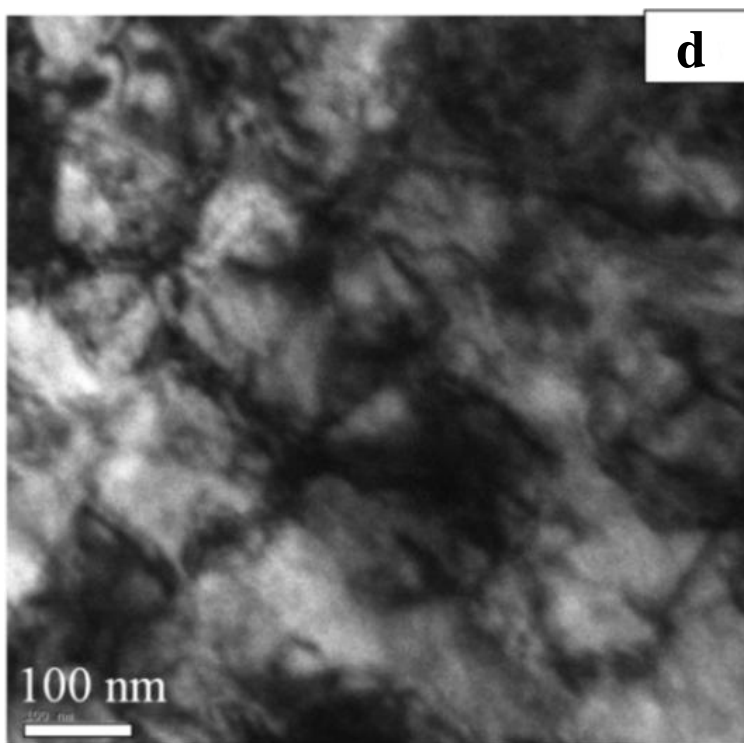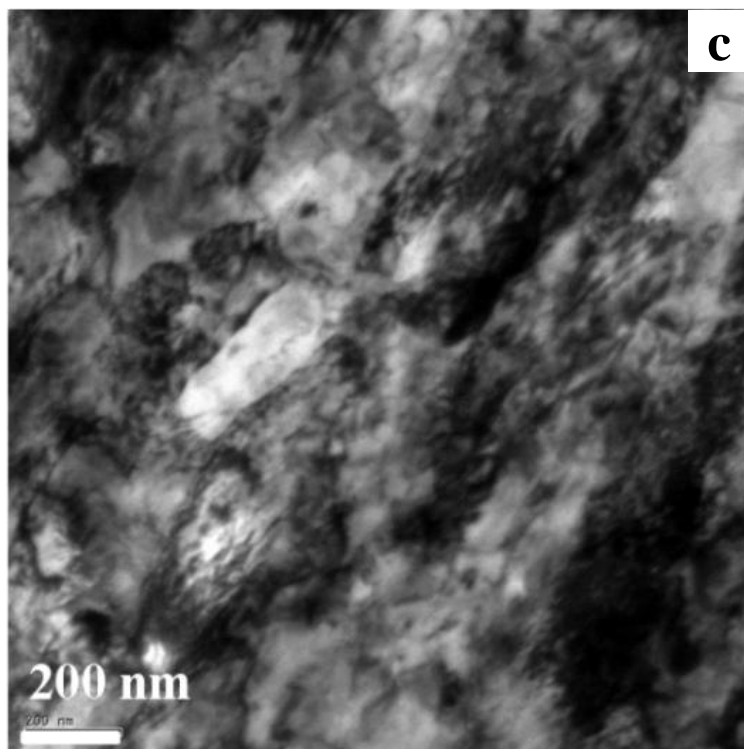**Figure 6.2:** TEM bright field images of (a) ECAP-12 and (b) ECAP-12-CR-90.

Figure 6.2: TEM bright field images of (c) ECAP-12-CRR-70 and (d) ECAP-12-CRR-96.

As-received IF steel consists of high fraction (88.4%) of sharply defined high angle grain boundaries (HAGBs) with misorientation angle spreaded over 15-62.8° (Figure 6. 4(a, g)), resulting in high average of misorientation (~37°) (Figure 6. 4(f), Table 6.1). At ε_{vm}=12, the misorientation plot shows that material is having majority of low angle grain boundaries (LAGBs) (~65.5%) and low fraction of HAGBs (34.5%) (Figure 6.4(g)), confirmed by misorientation distribution plot (Figure 6.4(b)) and low average misorientation angle (~15.8°) (Figure 6.4(f), Table 6.1). On further deformation of ECAPed sample by coldrolling to 90% (ECAP-12-CR-90) reduction in area, HAGB fraction increases to 58.3% (Figure 6. 4(e)), average misorientation angle increases to ~25° (Figure 6.4(f)). When the ECAPed material is cryorolled to 70% reduction in area (ECAP-12-CRR-70), HAGB fraction increases to 49.2% (Figure 6.4(d)) and average misorientation angle slightly decreases to 22.3° (Figure 6.4(f)) and significant amount of boundaries are having very low angle of misorientation (Figure 6.4(d)). In case of ECAP-12-CRR-96, fraction of HAGBs increases to ~60.8% (Figure 6.4(g)) with the distribution of high fraction of grains centered at misorientation angles of ~28.7° and 60° (Figure 6.4(e). Average misorientation angle increases to ~25.7° (Figure 6.4(f)).

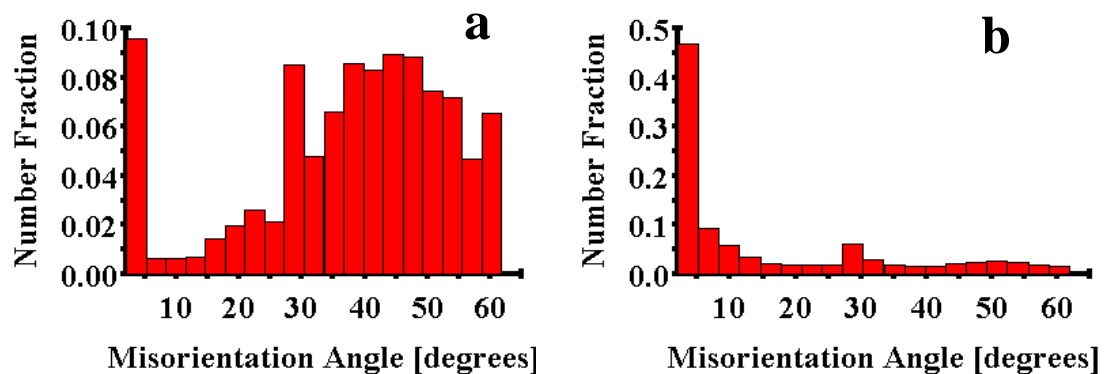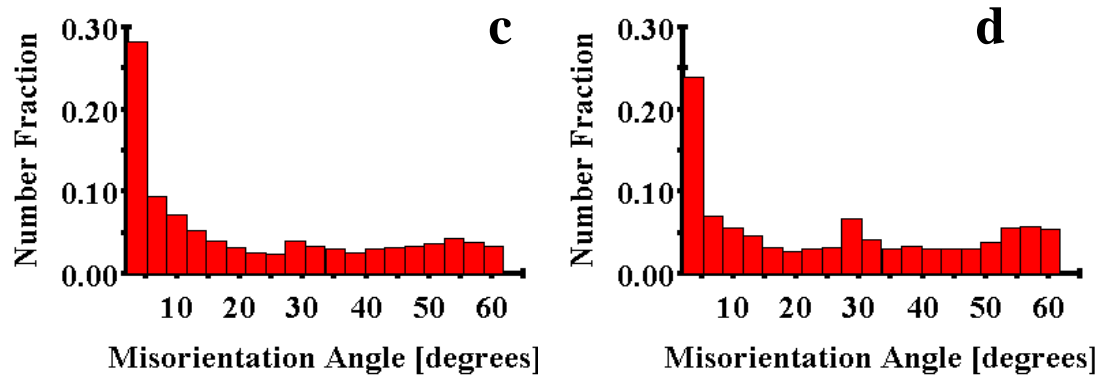**Figure 6.3:** Misorientation angle distribution of IF steel for (a) As-received, (b) ECAP-12.

Figure 6.3: Misorientation angle distribution for (c) ECAP-12-CR-90, (d) ECAP-12-CRR-70.
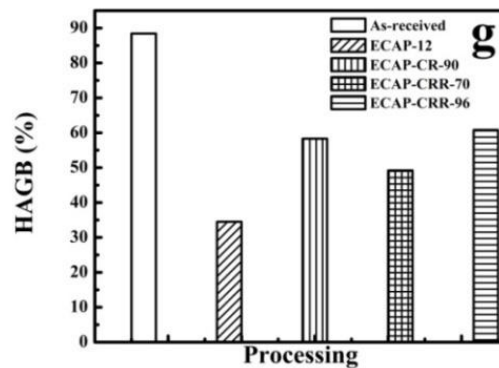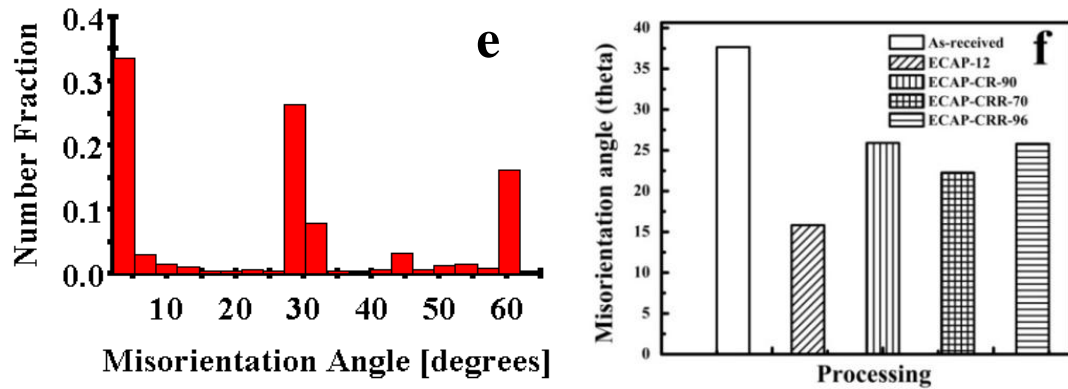
Figure 6.3: Misorientation angle distribution of IF steel for (e) ECAP-12-CRR-96 IF steels, (f) variation of average misorientation angle and (g) HAGB fraction with respect to processing condition of material.

135

6.2 Texture Evolution

The Φ_2=45° section of the ODF plots of ECAP-12-CR and ECAP-12-CRR samples is shown in Figures 6.4(a,b,c).

Figure 6.4: $\Phi2$=45° ODF maps of IF steel after ECAP for (a) ECAP-12-CR-90, (b) ECAP-12-CRR-70, (c) ECAP-12-CRR-96.

The ODFs show the presence of RD and ND fibers. The ND fiber is equally strong in ECAP followed by cryorolling states, while the RD fiber seems to be stronger in

ECAP followed by coldrolling state. If both cryorolled states are compared (Figures 6.4(b,c)), one observes strong ND fiber in ECAP-12-CRR-96 sample compared to ECAP-12-CRR-70 sample. Main components of rolling fiber i.e. $\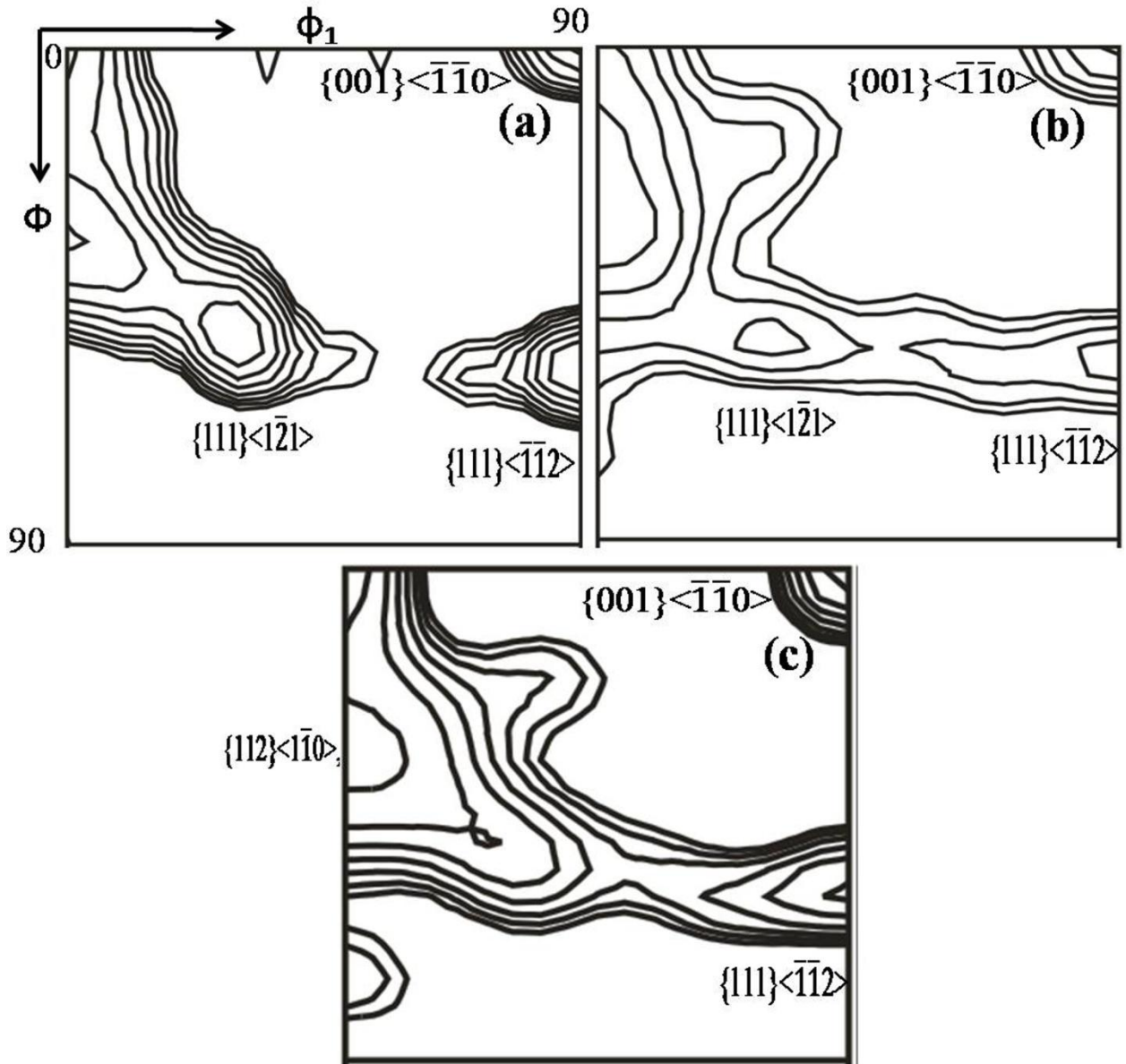{112\}<1\bar{1}0>$, $\{111\}<\bar{1}\bar{1}2>$ and $\{111\}<1\bar{2}1>$ are existing in ECAP-12-CRR-70 with strong RD fiber. Along with these components $\{001\}<\bar{1}\bar{1}0>$ component is also existing. The RD fiber (Figure 6.4(c)) shows equally strong peaks at $\{112\}<1\bar{1}0>$ and $\{001\}<1\bar{1}0>$ with ND fiber at $\{111\}<\bar{1}\bar{1}2>$ in ECAP-12-CRR-96. In all the deformed states i.e. ECAP-12-CR-90 (Figure 6.4(a)) and ECAP-12-CRR-70, ECAP-12-CRR-96 samples (Figures 6.4(b,c)), strong component of cube texture $\{001\}<\bar{1}\bar{1}0>$ are observed.

6.3 Mechanical Properties

As-received IF steel is having low hardness value of 174±7.5 VHN (Table 6.2). Upon ECAP (ε_{vm}=12), the hardness increases to 300±3 VHN (Table 6.2). On further coldrolling of ECAPed IF steel (ECAP-12-CR-90), hardness improved to 524±25 VHN. Further increase in hardness is only marginal when the ECAPed samples are subjected to cryorolling to 96% reduction in area (only to 530.3±0.5 VHN) (Figure 6. 3).

The as-received coarse grained IF-steel exhibits low yield strength of 227 MPa but appreciable tensile strength of 337 MPa with large amount of uniform elongation (26%) and total elongation (41.8%) (Figure 6.5 and Table 6.2). After ECAP for ε_{vm}=12, yield increases by 3.5 times and tensile strength improves by 2.5 times due to refinement to ultrafine level but uniform elongation reduces to 2.2% and total elongation becomes 16.2%. Upon coldrolling of ECAPed IF steel to 90% reduction in area yield strength further increases by 1.4 times and tensile strength significantly but ductility decreases. The yield strength of cryorolled sample is higher than that of cold rolled sample.
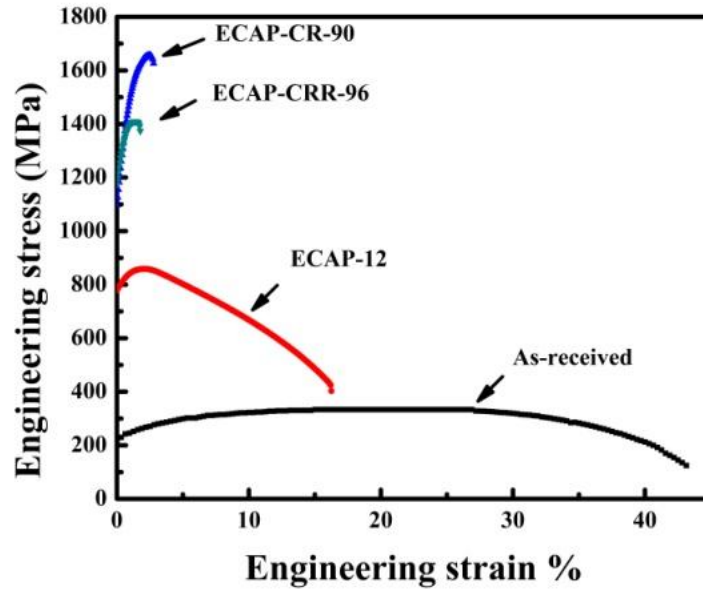
Figure 6.5: Engineering stress-strain curves of IF steel samples.

Table 6.2: Mechanical properties of post ECAPed deformed IF steel samples

Sample	Yield Strength (MPa)	Ultimate Tensile Strength (MPa)	Uniform Elongation (%)	Total Elongation (%)	Hardness (VHN)
As-received	227	337	26	41.8	174±7.5
ECAP-12	795	859	2.2	16.2	300±3
ECAP-12-CR-90	1104	1657	2.5	2.8	524±25
ECAP-12-CRR-70	595	1149	12.4	15.6	390.7±4.3
ECAP-12-CRR-96	1195	1409	1.5	1.7	530.3±0.5

6.4 Fractography

Figure 6.6 shows brittle fracture surface of ECAP-12-CR-90, ECAP-12-CRR-70 and ECAP-12-CRR-96 samples.
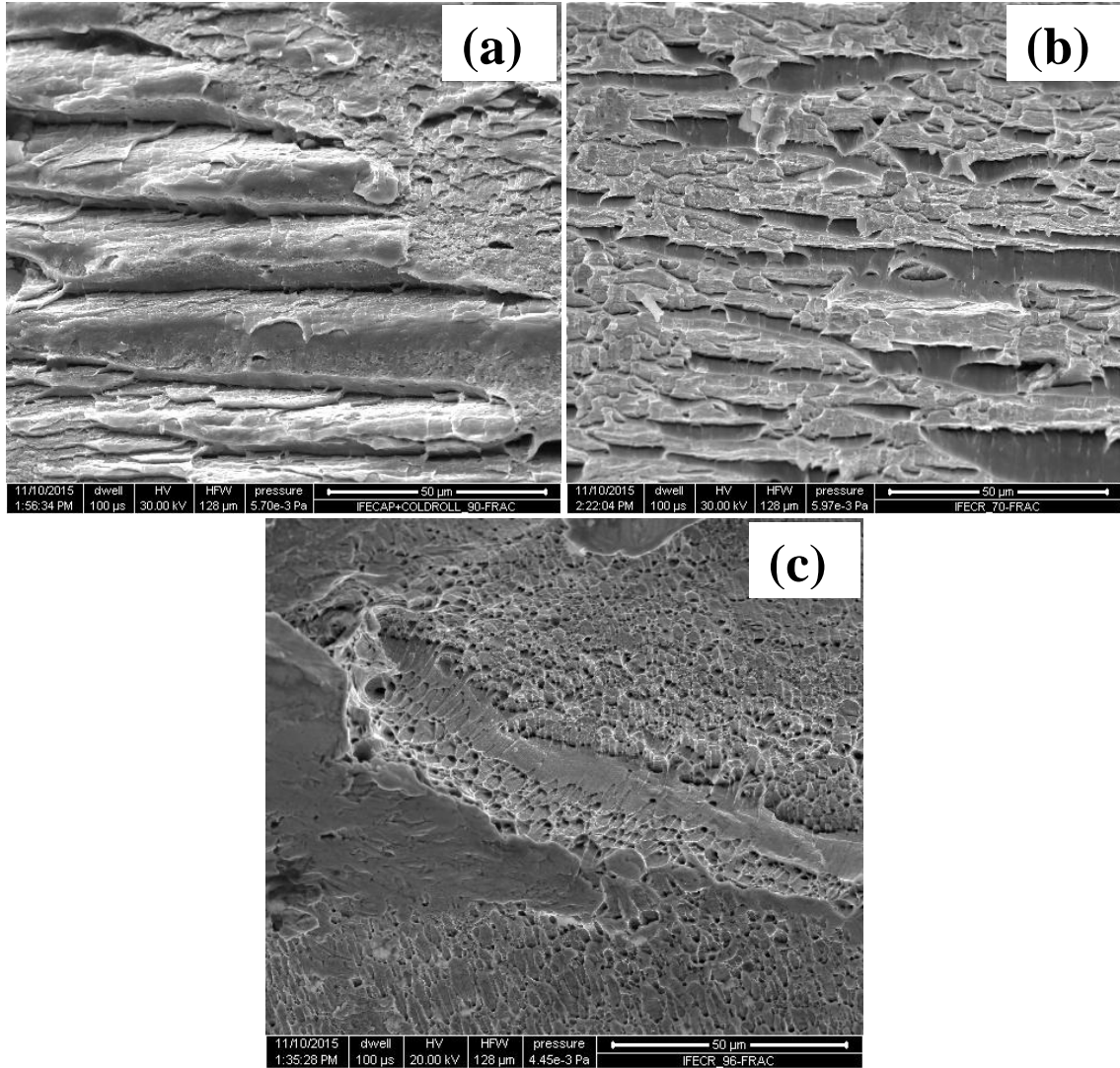
Figure 6.6: Microstructure of fracture surface of IF steel of (a) ECAP-12-CR-90, (b) ECAP-12-CRR-70, (c) ECAP-12-CRR-96.

6.5 Discussion

The samples subjected to ECAP at $\varepsilon_{vm}=12$ show high fraction of low angle grain boundaries (LAGBs) (Figure 6.3(b)) and the low value of average misorientation angle (Figure 6.3(f)) which suggest that dislocations are rearranged in the form of cell walls leading to the reduced domain size due to the dynamic recovery processes (Figure 6.2(a)). However, the samples still possess a high elastic stored energy (Table 6.1) due to the presence of a large number of scattered dislocations (Figure 6.1(b)), small cell size

(Table 6.1) and high amount of lattice strain. When ECAPed material is further coldrolled or cryorolled, it is expected that elastic stored energy increases due to the generation and the propagation of additional dislocations as well as morphological changes of the grains. When ECAPed material is coldrolled (ECAP-12-CR-90) it may become difficult to pump in more dislocations into the grain interior as the microstructure is already in dynamically recovered state but subgrains begin to rotate in the direction of deformation together with the dynamic recovery processes (Figure 6.1(b)). During deformation some part of energy is stored in the material as dislocations and the other part is dissipated as heat which causes dynamic recovery [Hodowany et al. 2000]. Dynamic recovery results in well arranged dislocations in the form of the cell walls and the dislocation tangles (Figure 6.2(b)) with further reduced domain size. The large value of elastic strain energy is related to the scattered dislocation density, the cell formation (Figure 6.2(b)) and the residual microstrain. Due to dynamic recovery the cell walls begin to form subgrains and consequently the dislocations within subgrains are annihilated. The long range internal stresses are associated with these cell walls and its interior [Kostorz et al. 2013]. Cryorolling of the ECAPed sample is another way of pumping a large number of dislocations as mobility of dislocations is restricted due to lower temperature of deformation.

A high amount of dislocations are accumulated and thereby the immobile dislocations reach to a saturation level [Hertzberg et al. 1996, Wang et al. 2003]. The 70% cryorolled sample (ECAP-12-CRR-70) showed the deformation induced subgrain rotation towards a new orientation and their coalescence (Figure 6.1(c)) that is associated with increase in elastic stored energy. A consistent increase in average misorientation

angle also occurs (Figure 6.3(f)) in comparison to the ECAPed (ECAP-12) sample. Zhang et al. [Zhang et al. 2005] have reported that cryogenic deformation is a stress driven process similar to the grain growth which is also observed during nanoindentation resulting from subgrain boundary migration, grain rotation and coalescence [Jin et al. 2004]. The dislocations move towards the grain boundaries (Figure 6.1(c)), setting up long range elastic stresses due to the interaction of the lattice dislocations with the grain boundaries, as observed in Figure 6.1(h), and due to the difficulty of accommodation of differently oriented grains [Sauvage et al. 2012], dislocations are appearing at grain boundaries making thick boundary walls. The extinction contours are also visible within and at the grain boundaries (Figure 6.2(c)). These extinction contours are indicative of the nonequilibrium state of the grain boundaries as a consequence of high internal stress [Park et al. 2000, Wang et al. 1996, Hodgson et al. 1999]. The nonequilibrium grain boundaries are those having highly distorted crystallite lattice in ultrafine-grained materials [Nazarov et al. 1993]. The distribution of misorientation angle (Figure 6.3(d)) shows that a large fraction of these boundaries is arranged in the form of low angle configuration.

Further cryogenic deformation of 96% reduction in area of IF steel (ECAP-12-CRR-96) leads to the refinement of the grains (Table 6.1) and increase in elastic stored energy (Table 6.1) compared to ECAP-12-CR-90 sample due to a large number of scattered dislocations. The boundaries of grains are diffuse which confirm nonequilibrium state of these boundaries (Figure 6.2(d)). The EBSD map also confirms the existence of heterogeniety in the material (Figure 6.1(d)). Increase in hardness of ECAPed material in comparison to the as-received material is due to the decrease in grain

size (Figure 6.2(a)) and due to a large number of dislocations. Further increase in hardness after changing the mode of deformation from ECAP to rolling is due to the combined effect of increased fraction of HAGBs (Table 6.1) and large number of scattered dislocations. When ECAPed material (ECAP-12-CR-90) is coldrolled, the yield strength increases further due to lower grain size (Figure 6.1(g)), higher dislocation density and increased misorientation angle (Table 6.1) in comparison to ECAPed material. On cryorolling the strength improves further due to the higher dislocation content (Figure 6.2(d)). ECAP, ECAP+cold rolling/cryorolling results in the ultrafine-grained microstructure in IF steel. The lack of dislocation interactions due to the reduced grain size in UFG microstructure produces a very low strain hardening rate. As a result the plastic instability occurs at very early stages of tensile testing displaying a limited uniform elongation [Purcek et al. 2012].

Results of Pole Figures show that there is difference in texture when ECAP is followed by coldrolling and cryrolling of material. Even though grains get elongated in the rolling direction when ECAPed material is coldrolled or cryorolled, formation of different texture components take place. Deformation texture forms by rotation of grains to a stable orientation from unstable state [Humphreys et al. 1995, Ray et al. 1994, Verlinden et al. 2007]. $\{112\}<1\bar{1}0>$ of α fiber and $\{111\}<\bar{1}\bar{1}2>$ of γ fiber are stable orientations. There is a weak texture in ECAP followed by cryorolled to 70% reduction in area while orientation density increased and a strong γ fiber is developed in ECAP-12-CRR-96. Brittle fracture surface of ECAP-12-CR-90, ECAP-12-CRR-70 and ECAP-12-CRR-96 samples is indicative of resistance to slip or plastic deformation. In case of ECAP-12-CR-90 sample splits are visible in parallel direction to each other. The

formation of these delaminations is expected to be due to elongated grain shape, texture, decohenson of grain boundaries and aligned particles [He 2013].

6.6 Summary

The post ECAP deformation of IF steel by cold rolling/cryorolling to 90% reduction in area decreases the grain size and improves the area fraction of high angle grain boundaries. When ECAPed IF steel samples are cryorolled heavily stressed non-equilibrium grain boundaries are formed. The enhancement in high angle grain boundary fraction, the nonequilibrium boundaries and the reduction in grain size strengthen the material significantly. Decrease in grain size to ultrafine levels with increased lattice strain lowers the work hardening ability of the steel and consequently limits its ductility. Texture results show that changing mode of deformation from ECAP to cryorolling leads to formation of γ fiber. Whereas, no sharp γ fiber is formed by coldrolling of ECAPed material.